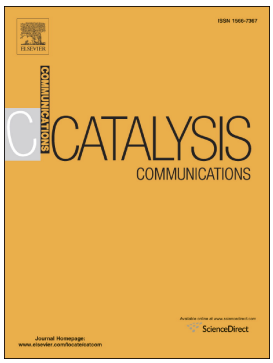

Sulphur tolerant diesel oxidation catalysts by noble metal alloying

Tanja Franken, Elisabeth Vieweger, Andreas Klimera, Michael Hug, Andre Heel

PII: S1566-7367(19)30194-3
DOI: https://doi.org/10.1016/j.catcom.2019.105732
Article Number: 105732
Reference: CATCOM 105732

To appear in: *Catalysis Communications*

Received date: 21 March 2019
Revised date: 13 June 2019
Accepted date: 18 June 2019" role="suppressed

Please cite this article as: T. Franken, E. Vieweger, A. Klimera, et al., Sulphur tolerant diesel oxidation catalysts by noble metal alloying, Catalysis Communications, https://doi.org/10.1016/j.catcom.2019.105732

Sulphur tolerant diesel oxidation catalysts by noble metal alloying

Tanja Franken[1], Elisabeth Vieweger[2], Andreas Klimera[2], Michael Hug[2], Andre Heel[1]

[1] Zurich University of Applied Sciences (ZHAW), Institute of Material and Process Engineering (IMPE), Technikumstrasse 9, CH-8401 Winterthur, Switzerland.

[2]Hug Engineering AG, Im Geren 14, CH-8352 Elsau, Switzerland.

Abstract

A series of Mn-alloyed Pt supported catalysts were investigated for the NO oxidation reaction applied in diesel oxidation catalysts under sulphur-containing conditions. The observed NO oxidation conversion correlated to the Pt amount in the catalyst under sulphur-free conditions. In the presence of SO_2 in the feed, the Pt/Al_2O_3 catalyst heavily deactivated resulting in the lowest performance compared to Mn-alloyed Pt catalysts. Already small amounts of Mn improved the SO_2-resistance significantly. Whilst pure Pt/Al_2O_3 catalyst deactivates fully within the first 30 min under NO oxidation conditions including 300 ppm SO_2, an alloy with a Mn to Pt ratio of 1:1 performed with a remarkable high catalytic stability for the NO oxidation over at least 70 h under continuous testing conditions.

Keywords: Sulphur tolerance, NO oxidation, Mn-Pt alloy, deNOx, manganese, platinum.

1. Introduction

An effective exhaust gas aftertreatment of diesel engine is indispensable to decrease the emissions of greenhouse gases and those of health-affecting, especially in cities of developing countries with increasing individual traffic. Typically, these aftertreatment systems consist of three stages, namely: the diesel oxidation catalyst (DOC), the catalysed soot filter (CSF), and the selective catalytic reduction (SCR). The main function of the DOC is the total oxidation of CO, unburned hydrocarbons (HCs) and oxidation of NO to NO_2 [1, 2]. Even though NO_2 is hazardous to human and environment, its presence in the exhaust significantly reduces the temperature for a continuous regeneration of the CSF and increases the NO reduction efficiency in the SCR unit [3-5]. Industrial applied DOC mainly consist of supported Pt or Pt-Pd-catalysts on Al_2O_3 [6-8]. Their fast deactivation in the presence of sulphurous gases such as SO_2 in the engine exhaust gas is a ubiquitous drawback of these catalysts. Due to the effective desulfurization process of diesel fuel in the EU among other countries, deactivation of Pt and Pt-Pd by sulphur poisoning is only a minor issue. Still nowadays, a comprehensive availability of sulphur-free gasoline is not available in many developing and emerging countries. Hence, if the DOC is poisoned by SO_2 by using high sulphur loaded fuel, the catalyst is irreversibly deactivated and loses its function. An insufficiently working DOC leads to pore blocking of the CSF by soot and a diminished SCR efficiency. Thus, the whole emission aftertreatment system loses its function completely.

A typical challenge of Al_2O_3-supported catalysts is the formation of $Al_2(SO_4)_3$ due to reaction with SO_2 [9] that limits the catalytic activity and stability of Al_2O_3-supported catalysts by altered surface physico-chemical properties [10, 11]. Non-sulphating supports such as SiO_2, ZrO_2, CeO_2 and mixtures thereof were investigated to improve the SO_2 tolerance, which lead to minor improvements [9]. During adsorption, SO_2 decomposes either spontaneously or thermally induced on most of the metal surfaces [12]. The interaction of S with Pt induces perturbations of the Pt electronic environment in the form of charge transfer from Pt 5d valence states to S and a rehybridization of the Pt (5d,6s,6p) orbitals [13]. These perturbations have a long range character in such a way that one sulphur atom can deactivate 10 or more equivalent metal sites [14].

Modification of the metal electronic environment is conceivable to overcome the electronic perturbations induced by S. This is possible via metal alloying due to the ligand effect in metal-metal bonding, which modifies the chemical affinity of Pt for S. Concurrently,

bimetallic alloys generate a different environment on the catalyst by their ensemble effect, generating changes in the number of active sites present on the surface [15, 16].

Also, for other reactions suffering from SO_2 poisoning, such as the conversion of methane [17, 18] or V-free-SCR of NOx [19-21], the presence of manganese in these corresponding catalysts improves the SO_2 tolerance. Since the presence of Mn has a general positive influence on the SO_2 resistance, and Mn is additionally fully miscible with Pt [22], the present study investigates the performance of manganese-alloyed platinum catalysts supported on Al_2O_3 for the NO oxidation in the presence of SO_2.

2. Experimental

2.1. Catalyst preparation

All supported metal catalysts were prepared by the wet impregnation of amorphous aluminium oxide (Puralox TH 155, Sasol). In a typical synthesis, manganese acetylacetonate ($Mn(acac)_2$; Chempur) and platinum acetylacetonate ($Pt(acac)_2$; Chempur) were dissolved in 50 mL acetone according to the desired molar ratios in a range of Mn:Pt of 3:1 to 0:1. The total molar amount of metal (n(Mn) + n(Pt)) was fixed for all catalysts to the molar amount of platinum corresponding to a 3 wt% Pt loading for the reference catalyst (no Mn loading). The molar amount of total metal was fixed in order to have always the same number of metal atoms on the surface of the support. As Pt has a much higher molar weight than Mn, a fixed mass loading would result into different number of total metal atoms impregnated on the support. After dissolution of metal precursor salts, 2 g of aluminium oxide was added to the solution which was kept stirred for 24 h at 25 °C. Acetone was removed in a rotary evaporator at 40 °C under reduced pressure, ca. 560 mbar. The residual solid was dried for 12 h at 80 °C and subsequently calcined for 4 h in air at 650 °C (ramping 5 K/min).

2.2. Catalytic performance measurements

The NO oxidation performance of the catalysts was investigated in a fixed bed quartz glass micro-reactor at ambient pressure in the temperature range from 100 to 500 °C controlled with a K-type thermocouple inside the catalyst bed. Typically, 100 mg of pelletized catalysts (sieve fraction: 0.25 – 0.50 mm) were used as calcined, and the total flow of feed gas mixture was adjusted based on the catalyst bed height (0.9 – 1.1 cm) to obtain a GHSV of 120,000 h^{-1}

(total flow rate: 509 – 633 ml/min; catalyst volume: 0.254 – 0.311 cm^3). The feed gas reaction mixture was composed of 1000 ppm NO, 10 vol% O_2 and 300 ppm SO_2 (if needed) diluted in argon (inert balance gas). The outlet gas mixture was monitored via mass spectroscopy (Omnistar GDS 320, Pfeiffer, SEM detector), and effluent gas concentrations were obtained after suitable calibration of the mass spectrometer. The NO conversion was calculated according to Eq. (1):

$$X(NO) = \frac{c(NO_2)_{out}}{c(NO)_{in}} \qquad (1)$$

Eq. (1) considers that the molar flow rates of inlet and outlet gas mixture remain practically the same given the very low molar flow rate of NO present in the feed gas. No other nitrogen-containing gas products than NO_2 were observed during the NO oxidation tests. Stability tests were performed at a constant temperature, ca. 350 °C. The catalysts were heated and equilibrated in temperature in a flow of Ar gas. Each stability test was started by switching to the gas reaction mixture of 1000 ppm NO, 10 vol% O_2 and 300 ppm SO_2 diluted in Ar.

2.3. Catalysts characterization

X-Ray powder diffraction (XRD) patterns were recorded with Ni filtered Cu Kα radiation (1.5406 Å) on a Bruker D8 Advance diffractometer with a 2θ step sized of 0.2° from 10 to 110°. The metal surface area of the catalyst was measured via CO pulse titration on a Quantachrome Instruments Autosorb iQ TPX in dynamic mode, with an internal thermal conductivity detector and He as carrier gas. Prior to CO adsorption, the catalysts were reduced for 30 min in a gas mixture of 5 vol% H_2 in N_2 at 400 °C, and purged with He flow at 400 °C for further 30 min. After a cool down procedure in He gas flow, CO pulses were introduced with the internal and calibrated injection loop at the sample temperature of 40 °C. The adsorbed molar amount of CO was calculated by the ratio of missing peak area to full peak area, and analysed with the TPRWin software of Quantachrome Instruments. Specific surface area (S_{BET}) was measured by N_2 physisorption at the temperature of liquid N_2 in the same device using the p/p_0 range of 0.05 – 0.3, according to the BET theory.

3. Results and discussion

Porous Al_2O_3-supported MnPt catalyst were prepared with Mn:Pt ratios between 3:1 to 1:2 and compared with a 3 wt% Pt/Al_2O_3 (Mn:Pt = 0:1) catalyst for NO oxidation performance under SO_2-free and SO_2-containing gas conditions (Fig. 1 A, B). For a fully consistent set of data, all catalysts were prepared by keeping the total number of supported metal atoms the same. Hence, with increasing Mn content the Pt loading decreases from 3 wt% to 0.74 wt% (Table S1). Solid crystal phase analysis by powder XRD indicated that no secondary phases due to Mn incorporation existed, and diffraction peaks belong solely to the fcc crystal structure of metallic Pt (Fig. S1, S2). The diffraction peaks of this fcc phase shifted to lower diffraction 2theta angles (bigger lattice parameter) with increasing Mn content. This indicates the incorporation of Mn into the fcc phase of Pt by forming a Pt-Mn alloy phase. As expected, the pure Pt alumina-supported catalyst shows the highest low-temperature activity, and maximum conversion is reached at the lowest temperature, ca. 300 °C under SO_2-free NO oxidation reaction conditions (Fig. 1A). Accordingly, the temperature of maximum conversion increases with decreasing Pt loading or increasing Mn:Pt ratio. Surprisingly, all catalysts despite their substantially different Pt loadings exhibit full conversion, and the intrinsic activity per Pt-atom increases significantly with increasing Mn loading.

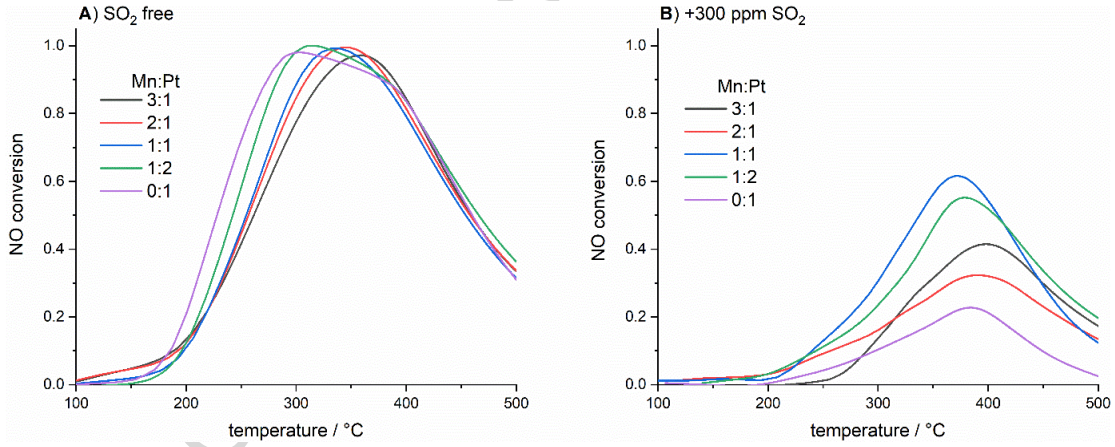

Figure 1: NO conversion vs. temperature profiles (100-500 °C) on $Mn:Pt/Al_2O_3$ catalysts without SO_2 (A) and with 300 ppm SO_2 (B) in the feed gas stream at GHSV of 120,000 h^{-1} in c(NO) = 1000 ppm; $c(O_2)$ = 10 % in Ar (gas balance).

As expected, NO oxidation experiments in the presence of 300 ppm SO_2 show that the 3 wt% Pt/Al_2O_3 catalyst results in a lower NO oxidation activity due to SO_2 poisoning. The NO conversion for Mn-alloyed Pt catalysts was also lower but to a less extent than Pt/Al_2O_3 (Fig. 1B). In fact, at all temperatures studied, nearly all Mn-contaning catalysts obtain higher NO conversions than the Pt/Al_2O_3 if SO_2 is present in the feed gas. Best performance of maximum

NO conversion of 60 % at 375 °C is observed with an equimolar ratio of Mn:Pt = 1:1. It has to be mentioned that in all catalytic tests under SO_2-load, oxidation of SO_2 to SO_3 takes place as a side reaction.

The catalytic activity itself does not correlate either to the amount of Mn or to the amount of Pt in the catalyst. Catalysts with a Mn content of 0.625 –0.41 wt%, the measured active metal surface area and the average particle size are in the same range of 0.35 – 0.55 m^2/g and 12 – 19 nm, respectively. Only the pure Pt and the 1:2 Mn:Pt catalyst have higher metal surface areas (ca. 1.3 m^2/g) and smaller particles sizes (ca. 5 nm) (Table S1). No CO uptake was detected upon the CO-pulse titration experiments conducted on pure Mn/Al_2O_3 catalysts. Hence, the measured MSA is assigned to the accessible Pt-metals surface area. Even though the 1:1 $Mn:Pt/Al_2O_3$ catalyst shows the lowest MSA, its NO oxidation performance in the presence of SO_2 is the highest. Dependent on the electronic properties of Pt, CO adsorbs in a bridged configuration on two neighbouring Pt sites [23]. Hence, the reduced MSA of this catalyst suggests a very high Pt dispersion and provides evidence for the presence of a Mn-Pt alloy phase. The S_{BET} of all catalysts are in the same range of 149 m^2/g, and mainly is defined by the S_{BET} of the Al_2O_3 support. Even though the textural properties of the Pt/Al_2O_3 and the 1:2 $Mn:Pt/Al_2O_3$ catalyst are very similar, the addition of small amounts of Mn amplified the catalytic NO oxidation activity in the presence of SO_2 to a significant extent.

The shift of diffraction peaks in the XRD and the altered CO adsorption indicated by the reduced MSA, suggest the creation of Pt-Mn alloy phase. According to the Mn-Pt phase diagram, alloying of the two metals is theoretically possible in all proportions. In addition, Mn:Pt-ratio of 3:1 creates a γ`-Mn_3Pt phase, 1:1 a β_1-MnPt and 1:2 a γ-$MnPt_3$ phases. Hence, the number of possible MnPt-pairs changes with composition, thus leading to a maximum in the formation of β_1-MnPt-phase [22]. With respect to the created alloy and corresponding phase diagram, a 50:50 mol% Mn:Pt-alloy (1:1 Mn:Pt) results in a β_1-PtMn-phase, wherein every Pt atom is fully co-ordinated by Mn and vice versa. The theoretical number of MnPt-pairs in the tested alloyed $MnPt/Al_2O_3$ catalysts, correlate with the observed NO oxidation activity in the presence of 300 ppm SO_2, indicating that the resistance to sulphur-poisoning is significantly improved by the presence of MnPt-pairs.

The high sulphur tolerance of the 1:1-$Mn:Pt/Al_2O_3$ catalyst was confirmed in a NO oxidation stability test in the presence of 300 ppm SO_2 under continuous operation at 350 °C

(Fig. 2). The 3 wt% Pt/Al_2O_3 catalyst shows high initial activity for a very short time, due to the exposure to SO_2 only. The high initial activity reflects the high activity of the non-poisoned catalyst, but the catalyst deactivates very fast and fully by sulphur poisoning within the first 30 min of the test (inset in Fig. 2). In contrast, the 1:1-Mn:Pt/Al_2O_3 catalyst shows very high catalytic stability for 70 h under a continuous SO_2 of 300 ppm. Besides the small fluctuations in activity appeared (Fig. 2), the average NO conversion decreases only slightly from 45 % to 39 % over the 70 h - stability test.

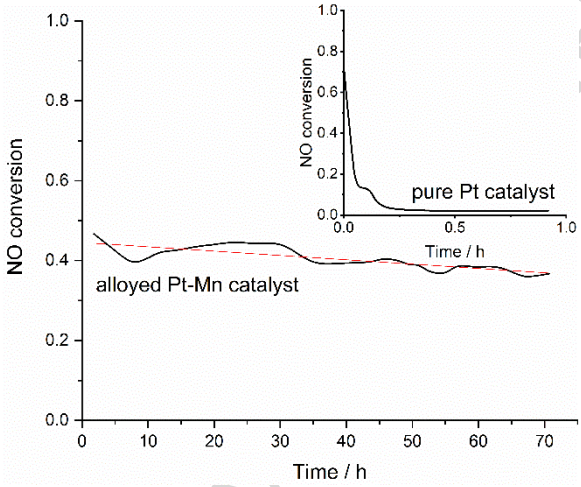

Figure 2: NO oxidation stability test at 350 °C conducted under continuous load of 300 ppm SO_2 on the 1:1-Mn:Pt/Al_2O_3 catalyst. Inset graph: Stability of 3 wt% Pt/Al_2O_3 as reference catalyst. Reaction conditions: GHSV = 120,000h^{-1}, c(NO) = 1000 ppm, c(O_2) = 10 vol%, c(SO_2) = 300 ppm in Ar at 350 °C.

4. Conclusions

Improved SO_2-resistance of Pt-based NO oxidation catalyst is obtained by alloying the expensive Pt noble metal with abundant Mn. Even though the catalytic activity decreases without SO_2 in the feed stream with increasing Mn content, both the activity and stability are significantly improved in the presence of SO_2, even with the addition of only minor amounts of Mn to the catalyst. The highest sulphur tolerance is obtained over the catalyst with equimolar amounts of Mn and Pt. Based on the phase diagram of PtMn alloy phases and theoretical assumptions, the improved SO_2-tolerance can be linked to the formation of MnPt-pairs formed by alloying present in the β_1 phase. The SO_2-tolerance correlates with the number of MnPt-pairs in the catalyst, and highest activity under SO_2 load as well as long-term

catalytic stability are observed in the catalyst with the highest number of such pairs. A thorough characterisation of the environment of active sites is challenging at this point due to the low concentration of active metal species (ca. 3 wt%) in the catalysts. Current research of the authors is focused on careful characterization and investigation of model catalysts to understand electronic perturbation within the alloy phase composition and the mechanism behind the improved sulphur tolerance.

Acknowledgements

The authors kindly acknowledge funding of the project NanoDOC by Innosuisse – Swiss Innovation Agency (project number: 18461.1 PFNM-NM).

References

[1] A. S. Ayodhya, K. G. Narayanappa, An overview of after-treatment systems for diesel engines, Environmental Science and Pollution Research 25 (35) (2018) 35034–35047.

[2] J. Lee, J. R. Theis, E. A. Kyriakidou, Vehicle emissions trapping materials: Successes, challenges, and the path forward, Appl. Catal. B: Environmental 243 (2019) 397 – 414.

[3] A. Setiabudi, M. Makkee, J. A. Moulijn, The role of $NO_2$and O_2 in the accelerated combustion of soot in diesel exhaust gases, Applied Catalysis B: Environmental 50 (3) (2004) 185–194.

[4] B. R. Stanmore, V. Tschamber, J.-F. Brilhac, Oxidation of carbon by NO_x, with particular reference to NO_2 and N_2O 87 (2008) 131 – 146.

[5] C. J. Tighe, M. V. Twigg, A. N. Hayhurst, J. S. Dennis, The kinetics of oxidation of diesel soots by NO_2, Combustion and Flame 159 (2012) 77 – 90.

[6] A. Morlang, U. Neuhausen, K. Klementiev, F.-W. Schütze, G. Miehe, H. Fuess, E. Lox, Bimetallic Pt/Pd diesel oxidation catalysts, Applied Catalysis B: Environmental 60 (3-4) (2005) 191–199.

[7] H. Dubbe, G. Eigenberger, U. Nieken, Modeling of conversion hysteresis phenomena for Pt/Pd-based diesel oxidation catalysts, Chemie Ingenieur Technik 90 (5) (2018) 625–633.

[8] M. Kaneeda, H. Iizuka, T. Hiratsuka, N. Shinotsuka, M. Arai, Improvement of thermal stability of NO oxidation Pt/Al_2O_3 catalyst by addition of Pd, Applied Catalysis B: Environmental 90 (3-4) (2009) 564–569.

[9] H. N. Sharma, S. L. Suib, A. B. Mhadeshwar, Interactions of sulfur oxides with diesel oxidation catalysts (DOCs), in: ACS Symposium Series, American Chemical Society, 2013, pp. 117–155.

[10] M. Konsolakis, I. Yentekakis, G. Pekridis, N. Kaklidis, A. Psarras, G. Marnellos, Insights into the role of SO_2 and H_2O on the surface characteristics and de-N_2O efficiency of Pd/Al_2O_3 catalysts during N_2O decomposition in the presence of CH_4 and O_2 excess, Applied Catalysis B: Environmental 138-139 (2013) 191–198.

[11] G. Corro, J. Fierro, R. Montiel, F. Bañuelos, Improved sulfur resistance of Pt-Sn/γ-Al_2O_3 catalysts for C_3H_8-NO-O_2 reaction under lean conditions due to Pt-Sn surface interactions, Journal of Molecular Catalysis A: Chemical 228 (1-2) (2005) 275–282.

[12] J. A. Rodriguez, J. Hrbek, Interaction of sulfur with well-defined metal and oxide surfaces: unraveling the mysteries behind catalyst poisoning and desulfurization, Accounts of Chemical Research 32 (9) (1999) 719–728.

[13] J. A. Rodriguez, M. Kuhn, J. Hrbek, The bonding of sulfur to a Pt(111) surface: photoemission and molecular orbital studies 251 (1996) 13 – 19.

[14] D. W. Goodman, Chemical modification of chemisorptive and catalytic properties of nickel, Application of Surface Science 19 (1984) 1 – 13.

[15] G. Ertl, H. Knötzinger, F. Schüth, J. Weitkamp (Eds.), Handbook of Heterogeneous Catalysis, 2nd Edition, Vol. 1, Wiley-VCH, New York, 1997.

[16] J. A. Rodriguez, D. W. Goodman, High-pressure catalytic reactions over single-crystal metal surfaces, Surface Science Reports 14 (1 -) (1991) 1 – 107.

[17] O. Buchneva, I. Rossetti, C. Oliva, M. Scavini, S. Appelli, B. Sironi, M. Allieta, A. Kryukov, L. Forni, Effective Ag doping and resistance to sulfur poisoning of La-Mn perovskites for the catalytic flameless combustion of methane, Journal of Materials Chemistry 20 (2010) 10021 – 10031.

[18] M. J. Koponen, T. Venäläinen, M. Suvanto, K. Kallinen, T.-J.-J. Kinnunen, M. Märkönen, T. A. Pakkanen, Methane conversion and SO_2 resistance of $LaMn_{1-x}Fe_xO_3$ (x = 0.4, 0.5, 0.6, 1) perovskite catalysts promoted with palladium, Journal of Molecular Catalysis A: Chemical 258 (2006) 246 – 250.

[19] J. Mu, X. Li, W. Sun, S. Fan, X. Wang, L. Wang, M. Qin, G. Gan, Z. Yin, D. Zhang, Enhancement of low-temperature catalytic activity over a highly dispersed FeMn/Ti catalyst for selective catalytic reduction of NO_x with NH_3, Industrial & Engineering Chemistry Research 57 (31) (2018) 10159–10169.

[20] C. Gao, J.-W. Shi, Z. Fan, G. Gao, C. Niu, Sulfur and water resistance of Mn-based catalysts for low-temperature selective catalytic reduction of NO_x: A review, Catalysts 8 (1) (2018) 11.

[21] J. S. Qiao, C. Y. Zhang, X. J. Yin, K. N. Sun, Study on performance of transition metal-doped catalysts for $DeNO_x$ at low-temperature, Advanced Materials Research 873 (2013) 612 – 618.

[22] H. Okamoto, M. E. Schlesinger, E. M. Mueller (Eds.), ASM-Handbook, Vol. 3, ASM International, The Materials Information Society, 1992.

[23] G. T. K. K. Gunasooriya, M. Saeys, CO adsorption site preference on platinum: Charge is the essence, ACS Catalysis 8 (5) (2018) 3770–3774.

Electronic Supporting Information

Tanja Franken[1], Elisabeth Vieweger[2], Andreas Klimera[2], Michael Hug[2], Andre Heel[1]

[1] Zurich University of Applied Sciences (ZHAW), Institute of Material and Process Engineering (IMPE), Technikumstrasse 9, CH-8401 Winterthur, Switzerland.

[2]Hug Engineering AG, Im Geren 14, CH-8352 Elsau, Switzerland.

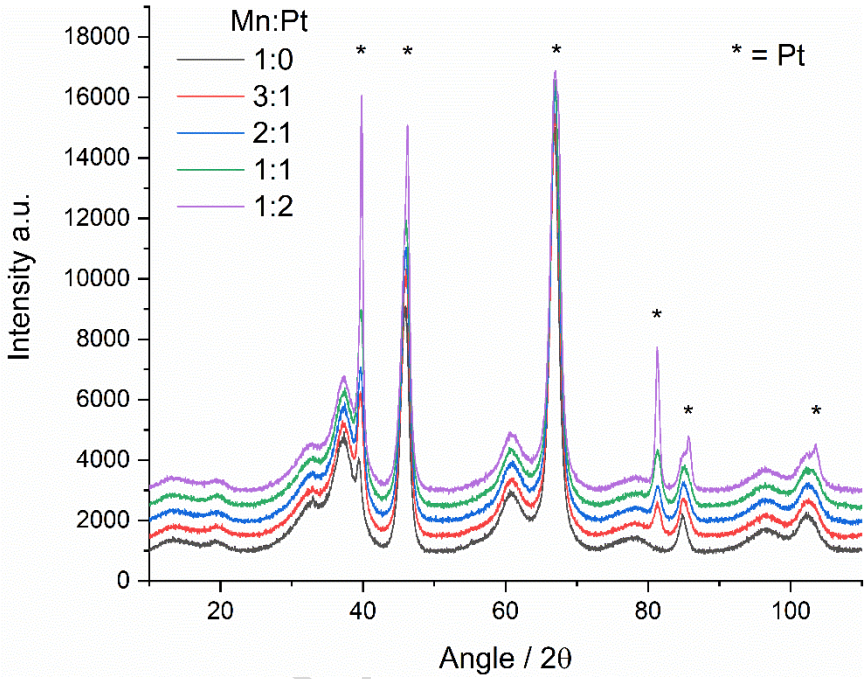

Figure S 1: Powder XRD of alloyed Mn:Pt-catalysts supported on amorphous Al_2O_3.

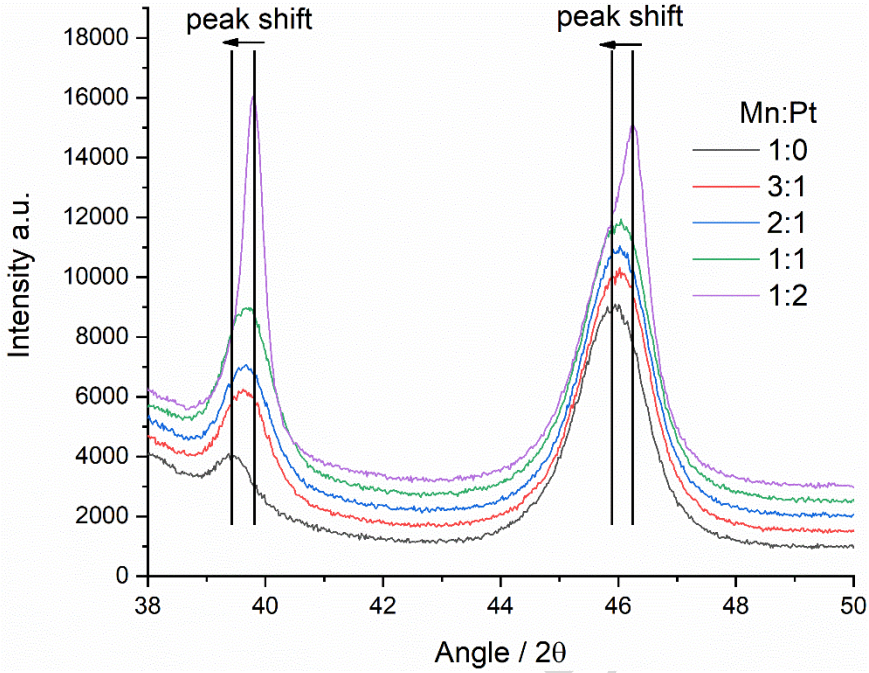

Figure S 2: Zoom of the XRD pattern illustrating the shift of diffraction peaks by the inclusion of Mn into the fcc-phase of Pt.

Table S 1: Overview of Pt and Mn wt% loading, metal surface area (MSA), average metal particle diameter (d_M) and specific surface area (S_{BET}) of catalysts with varying Mn:Pt-molar ratios supported on Al_2O_3.

Catalyst	Mn wt%	Pt wt%	MSA (m^2/g)	d_M (nm)	S_{BET} (m^2/g)
1:0 Mn:Pt	0.85	0	n.m	n.m	150.2
3:1 Mn:Pt	0.625	0.740	0.36	19.5	148.4
2:1 Mn:Pt	0.55	0.975	0.55	12.7	145.6
1:1 Mn:Pt	0.41	1.470	0.36	19.3	149.8
1:2 Mn:Pt	0.27	1.940	1.38	5.0	147.6
0:1 Mn:Pt	0.0	3.0	1.34	5.2	149.2

Highlights:

- Significant decrease of Pt loading by Mn alloying with minor decrease in performance
- Improved SO_2 tolerance by PtMn alloying
- Alloyed catalyst show substantial longer stability under continuous SO_2 feed

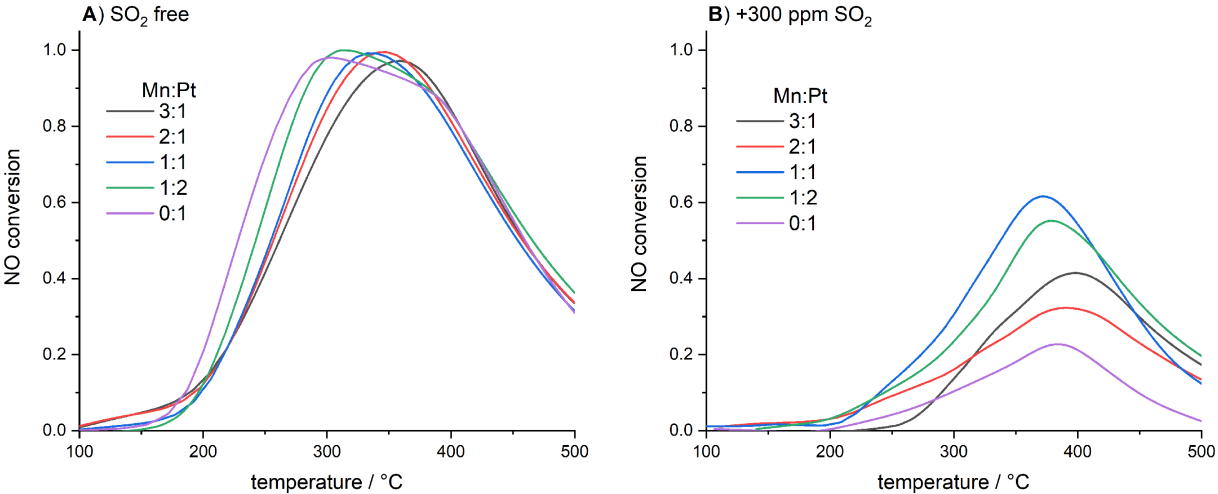
A) SO2 free
B) +300 ppm SO2
Mn:Pt
3:1
2:1
1:1
1:2
0:1
NO conversion
temperature / °C
0.0
0.2
0.4
0.6
0.8
1.0
100
200
300
400
500

Figure 1

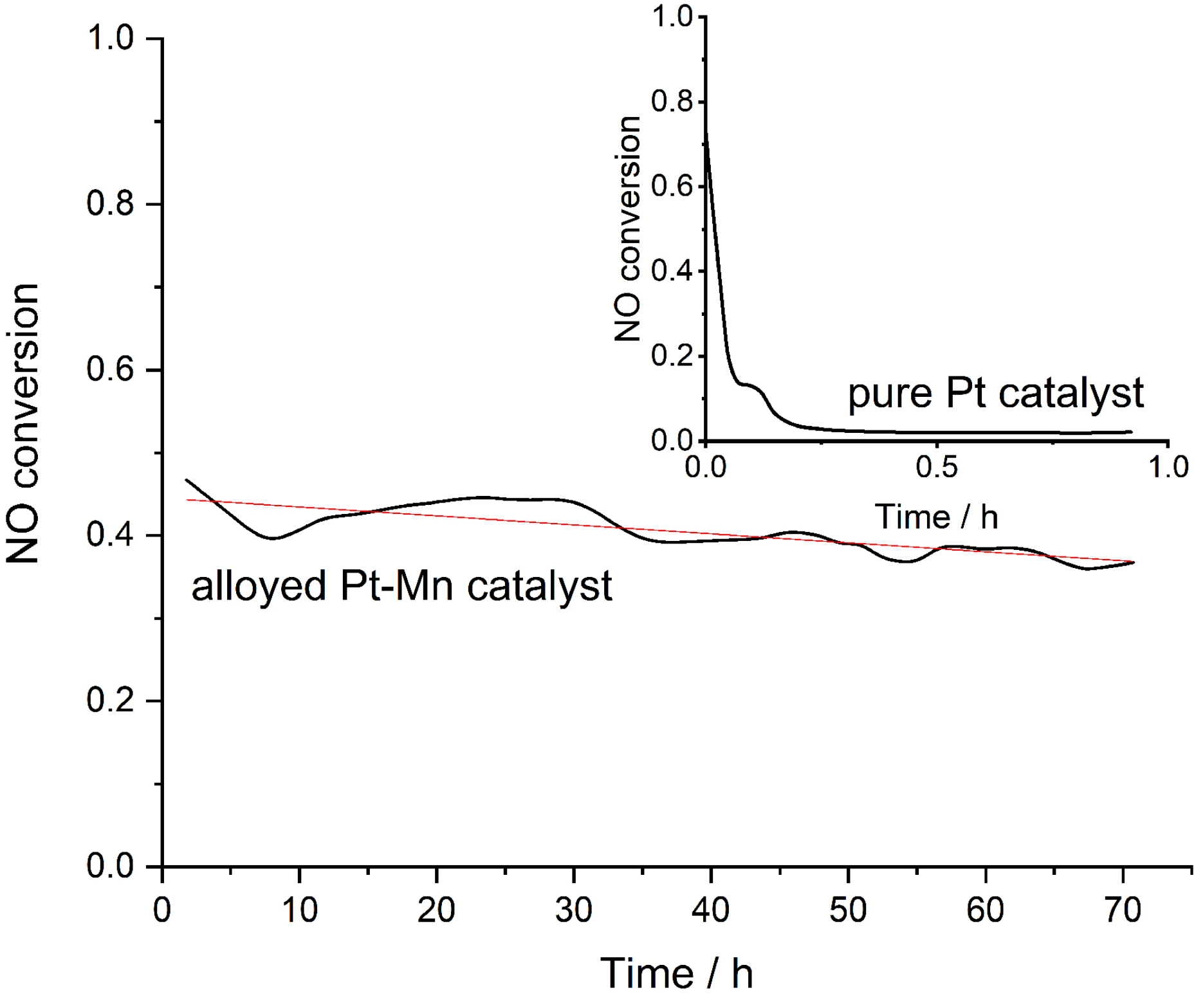
1.0
0.8
0.6
0.4
0.2
0.0
NO conversion
0
10
20
30
40
50
60
70
Time / h
alloyed Pt-Mn catalyst
1.0
0.8
0.6
0.4
0.2
0.0
NO conversion
0.0
0.5
1.0
Time / h
pure Pt catalyst

Figure 2